ORGANIC LETTERS

2003
Vol. 5, No. 7
1127−1130

The Change of Aromaticity along a Diels–Alder Reaction Path

Clémence Corminboeuf,*,† Thomas Heine,‡ and Jacques Weber†

Department of Physical Chemistry, University of Geneva, 30 quai Ernest-Ansermet, CH-1211 Genève 4, Switzerland, and Institut für Physikalische Chemie und Elektrochemie, TU Dresden, D-01062 Dresden, Germany

clemence.corminboeuf@chiphy.unige.ch

Received February 5, 2003

ABSTRACT

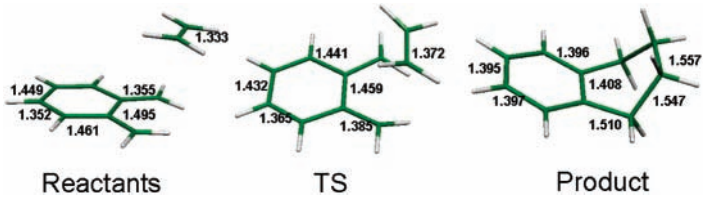

Quinodimethanes are highly reactive toward dienophiles since Diels–Alder cycloaddition results in an aromatic product. Density functional-based ^{13}C, ^{1}H NMR, NICS, and MO-NICS calculations indicate that the increase of aromatic character of the developing benzenoid ring along the reaction path is especially pronounced after the transition state is reached, even though the number of π orbitals decreases. The forming aliphatic ring exhibits large ring current effects during the reaction.

The well-known Diels−Alder reaction[1−8] is a standard method for forming substituted cyclohexenes through the cycloaddition of alkenes and dienes. The concerted nature of the mechanism and its stereospecificity were firmly established and are now well understood.[2,4,6−12]

The synthetic utility of the Diels−Alder reaction has been significantly expanded by the use and the developments of a wide variety of dienes and dienophiles that contain masked functionality.

Thus, *O*-quinodimethanes are exceedingly reactive because cycloaddition establishes a benzenoid ring, and results in aromatic stabilization.[13,14] Therefore, aromatization determines the energetically favorable reaction path.

The role of aromaticity in a set of Diels−Alder reactions involving *O*-quinodimethanes and their derivatives has already been studied by Manoharan et al.[15−18] and others.[19−22] Manoharan et al. showed that the aromatic character exhibited by the transition state and the product is responsible for both the kinetic and thermodynamic aspects of the reaction. Magnetic criteria such as magnetic susceptibility exaltation

† University of Geneva.
‡ TU Dresden.

(1) Butz, L. W. *Org. React.* **1949**, *5*, 136.
(2) Wassermann, A. *Diels−Alder Reactions*: *Organic Background and Physico-Chemical Aspects*; Elsevier: Amsterdam, The Netherlands, 1965; p 114.
(3) Patai, S., Ed. *The Chemistry of Alkenes* (*The Chemistry of Functional Groups*); Interscience: London, UK, 1964; p 1315.
(4) Sauer, J. *Angew. Chem., Int. Ed. Engl.* **1967**, *6*, 16.
(5) Marchand, A. P.; Lehr, R. E.; Editors. *Organic Chemistry, Vol. 35: Pericyclic Reactions, Vol. 1*; Academic: New York, 1977; p 286.
(6) Sauer, J.; Sustmann, R. *Angew. Chem.* **1980**, *92*, 773.
(7) Berson, J. A. *Tetrahedron* **1992**, *48*, 3.
(8) Winkler, J. D. *Chem. Rev.* **1996**, *96*, 167.
(9) Woodward, R. B.; Hoffmann, R. *Angew. Chem., Int. Ed. Engl.* **1969**, *8*, 781.
(10) Woodward, R. B.; Hoffmann, R. *The Conservation of Orbital Symmetry*; Academic: New York, 1970; p 178.
(11) Fleming, I. *Frontier Orbitals and Organic Chemical Reactions*; Wiley: London, 1976; p 258.
(12) Wollweber, H. *Diels−Alder Reaction*; Thieme: Stuttgart, Germany, 1972; p 270.
(13) Oppolzer, W. *Synthesis* **1978**, 793.
(14) Klundt, I. L. *Chem. Rev.* **1970**, *70*, 471.
(15) Manoharan, M.; De Proft, F.; Geerlings, P. *J. Org. Chem.* **2000**, *65*, 7971.
(16) Manoharan, M.; De Proft, F.; Geerlings, P. *J. Org. Chem.* **2000**, *65*, 6132.
(17) Manoharan, M.; De Proft, F.; Geerlings, P. *Perkin 2* **2000**, 1767.
(18) Manoharan, M.; Venuvanalingam, P. *J. Phys. Org. Chem.* **1998**, *11*, 133.
(19) Jursic, B. S. *Tetrahedron* **1997**, *53*, 13285.
(20) Jursic, B. S. *J. Chem. Soc., Perkin Trans. 2* **1995**, 1217.
(21) Chao, I.; Lu, H. F.; Chou, T. S. *J. Org. Chem.* **1997**, *62*, 7882.
(22) Di Valentin, C.; Freccero, M.; Sarzi-Amade, M.; Zanaletti, R. *Tetrahedron* **2000**, *56*, 2547.

10.1021/ol034203e CCC: $25.00
Published on Web 03/14/2003

(MSE)[23−25] and Nucleus Independent Chemical Shifts[26] (NICS) were used to evaluate the degree of aromaticity. In the present study we employ a refinement of NICS, the MO-NICS analysis,[27] which gives single MO contributions to NICS and thus provides a more detailed insight of the role of molecular orbitals during the aromatization process. The concept behind the analysis is discussed elsewhere[28] and the analysis has recently been applied to a series of organic rings and cages.[29] Geometry optimizations and frequency analysis were performed at the B3LYP/6-31G* level of theory. The reaction path was followed by using the Intrinsic Reaction Coordinate (IRC) type of calculation[30,31] as implemented in Gaussian 98.[32] MO-NICS[27] calculations were performed at the PW91/IGLOIII level using the GIAO[33] method as implemented in the MAG-ReSpect program.[34] NICS and MO-NICS values along the reaction path have been calculated at the center of the peripheral and at the average position of all six carbons of the forming ring.

The energy profile along the Diels−Alder reaction and the geometries at the most important steps along the IRC are displayed in Figure 1a. The activation barrier is found to be 8.2 kcal mol^{-1}. The product itself is 68.9 kcal mol^{-1} more stable than the reactants. These numbers are in very good agreement with those of Manoharan et al. (energy differences within 0.3 kcal mol^{-1}),[17] as well as are the geometries of reactants, product, and transition state. In more detail, the change of geometry along the IRC is as follows: First, the two π systems of the reactants are reacting in an endothermic process. The σ-bonds, which are forming the product from the reactant moieties, are established afterward. Relaxation of the sp^3 area of the molecule leads to the final structure, which is expressed by a twisting of the C−C bonds of the nonaromatic ring and bond length equalization of the benzenoid ring.

Changes in the magnetic susceptibilities and proton chemical shifts along the reaction paths of the Diels−Alder and closely related reactions were first reported in 1994,[35] and these studies were later extended to NICS and dissected (LMO) NICS analyses (see ref 21 in the related ref 17).

The progressions of NICS of the two rings are shown in Figure 1, parts b and c. For the "spectator" ring, the change of total NICS during the reaction is −11.6 ppm. It is interesting to note that NICS of the spectator ring is paratropic for the reactant, while it is turning to be diatropic at about the transition state. For the forming ring, the diatropic character is reaching a maximum at the transition state, as already discussed earlier.[17] These results show again[36−41] that NICS is a valuable index to demonstrate that the magnetic aromaticity is enhanced at the transition state. However, shortly afterward the NICS of the peripheral ring reaches a plateau phase, even though—as will be discussed below—the molecule is experiencing its largest transformations in structure, energetics, and electronic structure in this region. In contrast, the forming ring becomes highly diatropic at the transition state, and NICS only decreases afterward.[37]

The most obvious change, the formation of σ bonds between diene and dienophile, happens after the TS has been reached. According to the bond lengths equalization criterion the benzenoid ring (C1−C2 and C2−C3 bonds) is becoming aromatic at about step 100. Finally, the nonaromatic ring is transformed into the typical nonplanar sp^3 structure. NICS of the forming ring becomes very small. The restructuring stabilizes the molecule by 77.1 kcal mol^{-1} (Figure 1a).

The importance of the IRC part from the transition state to the product is also reflected in the ^{13}C and ^{1}H NMR patterns. In an aromatic ring, the ^{13}C and ^{1}H NMR chemical shieldings are usually close to those of benzene. Parts e and f of Figure 1 show the shieldings of all carbon and hydrogen atoms along the IRC. C_2 and C_3 differ by 10 ppm in the beginning. At the transition state they still differ by 8 ppm. Between the TS and the product, they then converge to the benzene value at about the same IRC step as the proton shifts (see H_2 and H_3 in Figure 1f) and the bond lengths of the benzenoid ring equalize (see structures in the abstract). The product $\delta(C_1)$ is shifted downfield with respect to benzene because of its central position. C_4 and C_5 transpose from sp^2 to sp^3 hybridization. This process starts at the transition state and finishes at the product, where the ^{13}C NMR values are in the typical sp^3 range. The proton shifts of the reactants are C-sp^2-H-like. During the reaction the outer protons of the nonaromatic ring become sp^3-like at the transition state. After the structural change, the inner protons of the aliphatic ring are shielded by the aromatic ring (Figure 1f).[37]

(23) Dauben, H. J., Jr.; Wilson, J. D.; Laity, J. L. *J. Am. Chem. Soc.* **1968**, *90*, 811.
(24) Schleyer, P. v. R.; Jiao, H. *Pure Appl. Chem.* **1996**, *68*, 209.
(25) Minkin, V. I.; Glukhovtsev, M. N.; Simkin, B. Y. *Aromaticity and Antiaromaticity*: *Electronic and Structural Aspects*; Wiley: New York, 1994; p 313.
(26) Schleyer, P. v. R.; Maerker, C.; Dransfeld, A.; Jiao, H.; Eikema Hommes, N. J. R. *J. Am. Chem. Soc.* **1996**, *118*, 6317.
(27) Corminboeuf, C.; Schleyer, P. v. R.; Heine, T.; Seifert, G.; Reviakine, R.; Seifert, G.; Weber, J. Submitted for publication.
(28) Corminboeuf, C.; Heine, T.; Weber, J. *Phys. Chem. Chem. Phys.* **2003**, *5*, 246.
(29) Moran, D.; Manoharan, M.; Heine, T.; Schleyer, P. v. R. *Org. Lett.* **2003**, *5*, 23.
(30) Gonzalez, C.; Schlegel, H. B. *J. Phys. Chem.* **1990**, *94*, 5523.
(31) Gonzalez, C.; Sosa, C.; Schlegel, H. B. *J. Phys. Chem.* **1989**, *93*, 8388.
(32) Frisch, M. J.; Trucks, G. W.; Schlegel, H. B.; Scuseria, G. E.; Robb, M. A.; Cheeseman, J. R.; Zakrzewski, V. G.; Montgomery, J. A., Jr.; Stratmann, R. E.; Burant, J. C.; Dapprich, S.; Millam, J. M.; Daniels, A. D.; Kudin, K. N.; Strain, M. C.; Farkas, O.; Tomasi, J.; Barone, V.; Cossi, M.; Cammi, R.; Mennucci, B.; Pomelli, C.; Adamo, C.; Clifford, S.; Ochterski, J.; Petersson, G. A.; Ayala, P. Y.; Cui, Q.; Morokuma, K.; Malick, D. K.; Rabuck, A. D.; Raghavachari, K.; Foresman, J. B.; Cioslowski, J.; Ortiz, J. V.; Stefanov, B. B.; Liu, G.; Liashenko, A.; Piskorz, P.; Komaromi, I.; Gomperts, R.; Martin, R. L.; Fox, D. J.; Keith, T.; Al-Laham, M. A.; Peng, C. Y.; Nanayakkara, A.; Gonzalez, C.; Challacombe, M.; Gill, P. M. W.; Johnson, B. G.; Chen, W.; Wong, M. W.; Andres, J. L.; Head-Gordon, M.; Replogle, E. S.; Pople, J. A. *Gaussian 98*, revision A.8; Gaussian, Inc.: Pittsburgh, PA, 1998.
(33) Ditchfield, R. *Mol. Phys.* **1974**, *27*, 789.
(34) Malkin, V. G.; Malkina, O.; Reviakine, R.; Schimmelpfennig, B.; Arbrouznikov, A.; Kaupp, M. MAG-ReSpect 1.0, 2001.
(35) Herges, R.; Jiao, H.; Schleyer, P. v. R. *Angew. Chem.* **1994**, *106*, 1441.
(36) Lecea, B.; Morao, I.; Cossio, F. P. *J. Org. Chem.* **1997**, *62*, 7033.
(37) Jiao, H.; Schleyer, P. v. R. *J. Phys. Org. Chem.* **1998**, *11*, 655.
(38) Morao, I.; Cossio, F. P. *J. Org. Chem.* **1999**, *64*, 1868.
(39) Cossio, F. P.; Morao, I.; Jiao, H.; Schleyer, P. v. R. *J. Am. Chem. Soc.* **1999**, *121*, 6737.
(40) Sawicka, D.; Wilsey, S.; Houk, K. N. *J. Am. Chem. Soc.* **1999**, *121*, 864.
(41) Sawicka, D.; Li, Y.; Houk, K. N. *J. Chem. Soc., Perkin Trans. 2* **1999**, 2349.

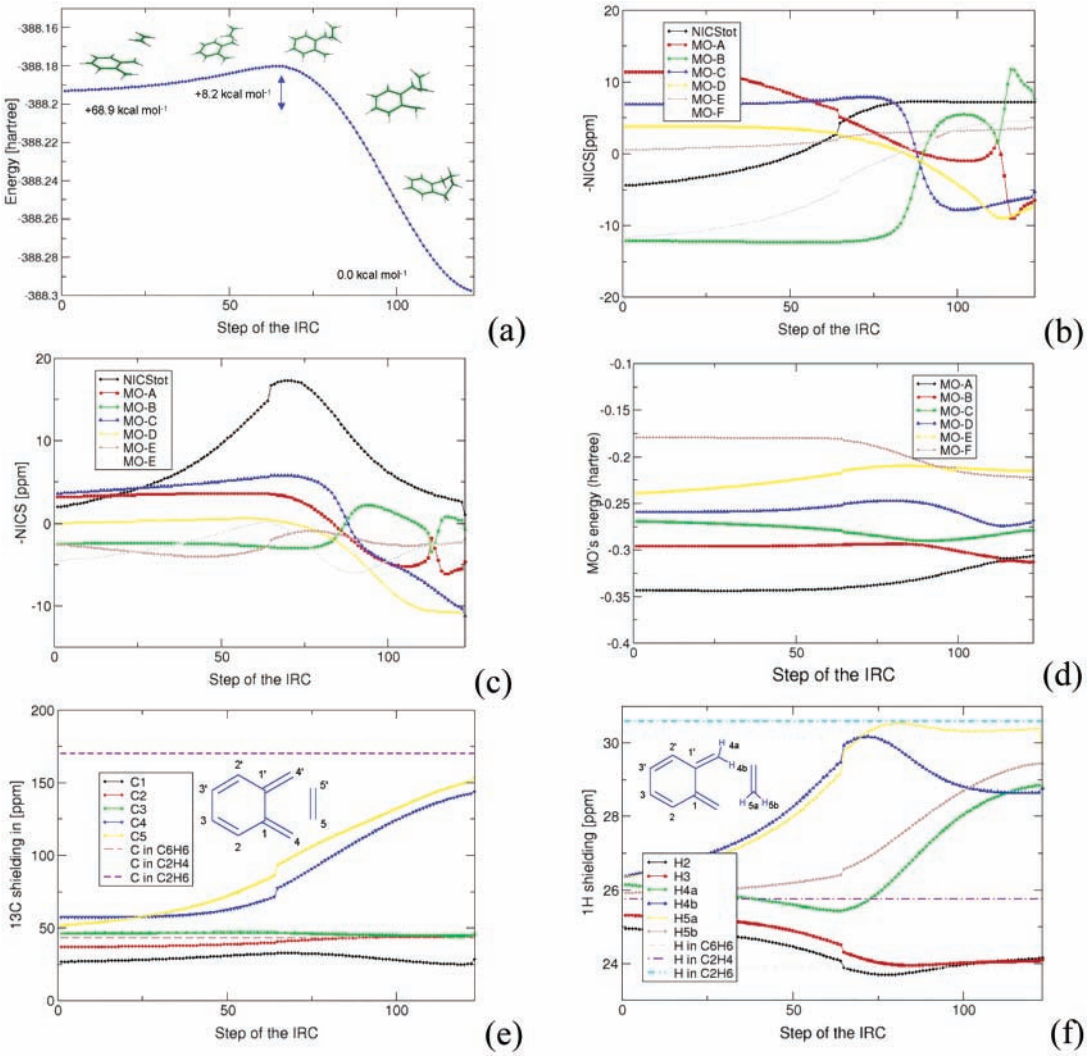

Figure 1. (a) Geometrical transformations and total energy changes along the IRC of the Diels−Alder reaction. MO-NICS analysis at the center of the peripheral (b) and forming (c) ring, (d) MO energies, (e) ^{13}C shielding, and (f) ^{1}H shielding. Orbitals are labeled as given in Figure 2.

The role of the π orbitals in the reaction is studied in terms of orbital shape, energies, and magnetic aromaticity contributions. The orbitals exhibiting π character during the reaction are displayed in Figure 2. Due to level crossings along the IRC, we label orbitals with letters (A to F). MO shapes change considerably during the reaction. Orbitals A, C, and D transform from π to σ character, while the symmetry of orbital B is changing from σ to π. Only two orbitals, E and F, keep their π character during the entire reaction. This observation was to be expected: there are five π orbitals in the reactants (MO's A, C, D, E, and F), while only three remain in the product (MO's B, E, and F). Typically, three π orbitals are involved in a Diels−Alder reaction. Two of them are coming from the diene while the third one belongs to the dienophile. In the product, two π orbitals are getting transformed into σ orbitals (MO's C and D), while the last π orbital is conserved (MO A/B).

Even though the number of π orbitals reduces along the IRC, the diatropicity of the peripheral ring of all π orbitals together increases (Figure 1b). The NICS$_\pi$ index[42] shows a considerable enhancement of π aromaticity in the final part of the IRC. As the number of π orbitals decreases from 5 to 3 in this part of the IRC a reliable number for NICS$_\pi$ can be given only for reactant (−11.2 ppm), transition state (−13.2 ppm) ,and product (−16.0 ppm). This implies that the diatropic character per orbital of the three final π orbitals is much higher than that for the five π orbitals of the reactants. However, the total change of NICS$_\pi$ is −4.8 ppm, a considerably smaller number than the change of NICS$_{tot}$ (−11.6 pm).

The modification of σ and π character of the orbitals is given by MO-NICS analysis.[27] At the peripheral ring center, all π orbitals are characterized by negative MO-NICS values. In other words, all π orbitals are found to be diatropic. On the other hand, the orbitals become paratropic as soon as

(42) Schleyer, P. v. R.; Jiao, H.; Eikema Hommes, N. J. R.; Malkin, V. G.; Malkina, O. *J. Am. Chem. Soc.* **1997**, *119*, 12669.

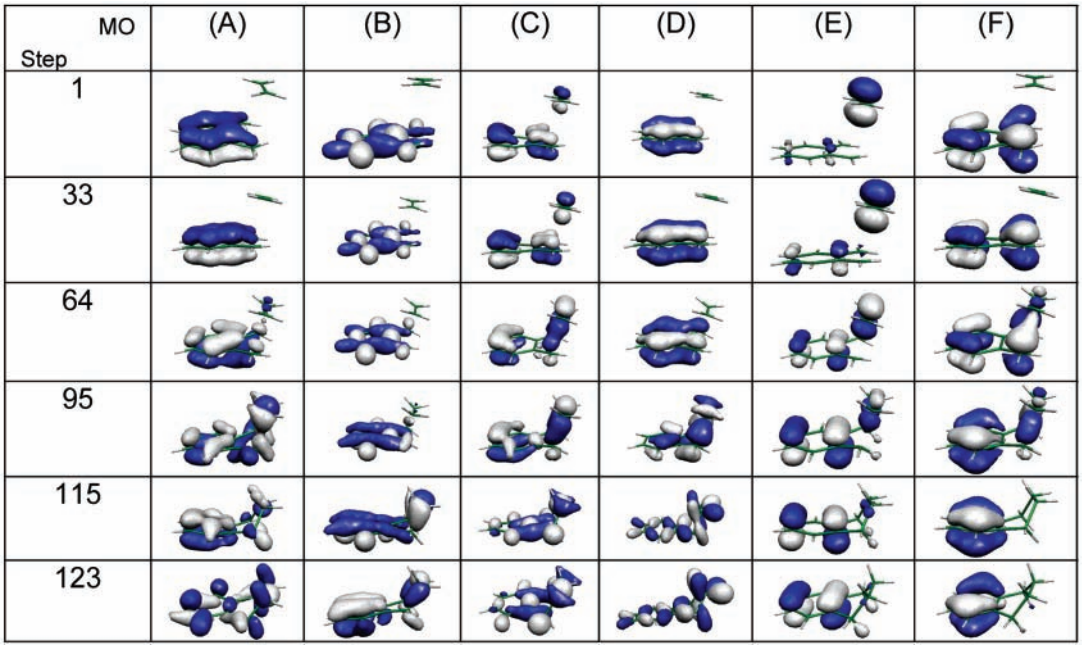

Figure 2. Molecular orbitals with π character during the Diels−Alder reaction at different steps of the IRC.

they exhibit σ character (see Figures 1b and 2). The largest changes of MO-NICS are found again between transition state and product. MO's E and F follow the same trend as NICS, but their MO-NICS contributions increase between the transition state and the product. MO's C and D alternate π into σ character and hence become paratropic in this region. Orbitals A and B have the strongest fluctuations along the IRC. They are transformed from σ to π and vice versa. The lowest π orbital is either A or B (Figure 2). In agreement with London−Hückel theory,[27,43] the lowest energy π orbital exhibits the highest contribution to MO-NICS.

MO-NICS also shows that the diatropicity of the forming ring at the transition state is attributed to the σ system ($NICS_\pi = -7.3$ ppm, see Figure 1c). The π MO-NICS contributions only decrease after the TS and there are no diatropic contributions from the π system at the product ($NICS_\pi = +5.1$ ppm).

At places of strong orbital mixing the MO-NICS values are hard to analyze. However, their main advantage in this context is that the contributions of π MO's can be seen clearly. The MO-NICS analysis complements nicely the other indices of aromaticity discussed here (NICS, $NICS_\pi$, ^{13}C, ^{1}H, bond length equalization). MO-NICS analysis also shows that the lowest energy π orbital is weakened during the reaction and reestablishes just before the product is reached. At this point MO B has a lower orbital energy than orbital A had for the reactant, and the orbital energy is further lowered for the product. All higher π orbitals are strongly influenced by this MO due to orthogonalization. Hence it plays a very important role during the reaction.

Beside the discussion of the Diels−Alder reaction it is worth noting that strong changes of MO-NICS are connected with those of orbital energy. The association of both quantities can be studied comparing parts b, c, and d in Figure 1. However, orbital energies and MO-NICS are not mathematically correlated.

Summarizing these results we can divide the IRC into three parts:

(i) The π orbitals of the ethylene dienophile overlap at the transition state. This overlap leads to the formation of an aromatic cycle C_1, C_2, C_3. C_2 and C_3 start to become benzene-like carbons (Figure 1d).

(ii) σ bonds are formed between the reaction partners. This is a continuous process between the transition state and the product: the large gain in binding energy and the increasing sp^3 character of the ^{13}C NMR shieldings of C_4 and C_5 are the best indication for this process. Also, the σ and π character of the MO's A−D is changing in this area.

(iii) The product structure is rearranged. In the last part of the IRC, the sp^3 framework of the C_3-C_5 ring takes on its typical nonplanar shape, as is visualized in Figure 1a. This goes along with rehybridization (Figure 2) and results in level crossings and strong changes in the MO-NICS analysis.

Acknowledgment. The authors want to thank the Swiss National Science foundation (20-63496.00/1) and the Graduiertenkolleg "Heterocyclen" of TU Dresden. We thank Alexei Arbouznikov and Roman Reviakine for the prerelease code distribution of a developer version of MAG-ReSpect 1.0 and Paul v. R. Schleyer for inspiring discussions.

OL034203E

(43) London, F. *J. Phys. Radium* **1937**, *8*, 397.